

tough on pathogens, safe on surfaces, huge convenience

Today more than ever, clinicians are turning to the disinfection power of Protex® from Parker Laboratories. Protex Disinfectant Spray and Protex ULTRA Disinfectant Wipes are highly effective for disinfecting and sanitizing hard, non-porous surfaces, killing SARS-CoV-2 (the virus that causes Covid-19) as well as HIV, H1N1 and MRSA.

Protex Disinfectant Spray, Ultra Disinfectant Wipes and now, Foaming Hand Sanitizer, come in several sizes to meet your facility's needs.

Protex Disinfectants. Protection for life.



proteX[®]
powerful • convenient • cost-effective • safe

Visit parkerlabs.com/protex for a complete list of uses.
Protex Ultra Disinfectant Wipes and Disinfectant Spray are not available in Europe.
Foaming Hand Sanitizer is not available in Europe or Canada.



Vinyl Exam
Tables



Transducers
& Probes



Mammography
Plates



Dental/Medical
Equipment



Hands
(sanitizer only)



Parker Laboratories, Inc.

The sound choice in patient care.™

973.276.9500

parkerlabs.com

ISO 13485:2016

A New Lung Ultrasound Protocol Able to Predict Worsening in Patients Affected by Severe Acute Respiratory Syndrome Coronavirus 2 Pneumonia

Tiziano Perrone, MD, PhD , Gino Soldati, MD, Lucia Padovini, MD, Anna Fiengo, MD, Gianluca Lettieri, MD, Umberto Sabatini, MD, Giulia Gori, MD, Federica Lepore, MD, Matteo Garolfi, MD, Iliara Palumbo, MD, Riccardo Inchingolo, MD, PhD , Andrea Smargiassi, MD, PhD , Libertario Demi, PhD , Elisa Eleonora Mossolani, MD, Francesco Tursi, MD, Catherine Klersy, MD, MSc, Antonio Di Sabatino, MD, PhD

Received September 15, 2020, from the Department of Internal Medicine, Fondazione Istituto di Ricovero e Cura a Carattere Scientifico, Policlinico San Matteo, University of Pavia, Pavia, Italy (T.P., L.P., A.F., G.L., U.S., G.G., F.L., M.G., I.P., A.D.S.); Service of Clinical Epidemiology and Biostatistics, Fondazione Istituto di Ricovero e Cura a Carattere Scientifico, Policlinico San Matteo, University of Pavia, Pavia, Italy (C.K.); Diagnostic and Interventional Ultrasound Unit, Valle del Serchio General Hospital, Lucca, Italy (G.S.); Pulmonary Medicine Unit, Department of Medical and Surgical Sciences, Fondazione Serhii Istituto di Ricovero e Cura a Carattere Scientifico, Policlinico Universitario Agostino Gemelli, Rome, Italy (R.L., A.S.); Department of Information Engineering and Computer Science, Ultrasound Laboratory Trento, University of Trento, Trento, Italy (L.D.); Emergency Medicine Unit, General Hospital Voghera, Voghera, Italy (E.E.M.); and Pulmonary Medicine Unit, Codogno Hospital, Azienda Socio Sanitaria Territoriale Lodi, Codogno, Italy (F.T.). Manuscript accepted for publication September 29, 2020.

We thank all the members of Accademia Di Ecografia Toracica, which were points of reference for constructive scientific discussions of clinical cases during the difficult period of the coronavirus 2019 pandemic. All of the authors of this article have reported no disclosures.

Address correspondence to Tiziano Perrone MD, PhD, Department of Internal Medicine, Fondazione Istituto di Ricovero e Cura a Carattere Scientifico, Policlinico San Matteo, Viale Camillo Golgi 19, 27100 Pavia, Italy.

E-mail: tperrone@smatteo.pv.it

Abbreviations

BMI, body mass index; CI, confidence interval; COVID-19, coronavirus disease 2019; CT, computed tomography; ICU, intensive care unit; LDH, lactate dehydrogenase; LUS, lung ultrasound; OR, odds ratio; SARS-CoV-2, severe acute respiratory syndrome coronavirus 2; US, ultrasound

doi:10.1002/jum.15548

Objectives—Severe acute respiratory syndrome coronavirus 2 (SARS-CoV-2) infection can generate severe pneumonia associated with high mortality. A bedside lung ultrasound (LUS) examination has been shown to have a potential role in this setting. The purpose of this study was to evaluate the potential prognostic value of a new LUS protocol (evaluation of 14 anatomic landmarks, with graded scores of 0–3) in patients with SARS-CoV-2 pneumonia and the association of LUS patterns with clinical or laboratory findings.

Methods—A cohort of 52 consecutive patients with laboratory-confirmed SARS-CoV-2 underwent LUS examinations on admission in an internal medicine ward and before their discharge. A total LUS score as the sum of the scores at each explored area was computed. We investigated the association between the LUS score and clinical worsening, defined as a combination of high-flow oxygen support, intensive care unit admission, or 30-day mortality as the primary end point.

Results—Twenty (39%) patients showed a worse outcome during the observation period; the mean LUS scores \pm SDs were 20.4 ± 8.5 and 29.2 ± 7.3 in patients without and with worsening, respectively ($P < .001$). In a multivariable analysis, adjusted for comorbidities (>2), age (>65 years), sex (male), and body mass index (≥ 25 kg/m²), the association between the LUS score and worsening (odds ratio, 1.17; 95% confidence interval, 1.05 to 1.29; $P = .003$) was confirmed, with good discrimination of the model (area under the receiver operating characteristic curve, 0.82). A median LUS score higher than 24 was associated with an almost 6-fold increase in the odds of worsening (odds ratio, 5.67; 95% confidence interval, 1.29 to 24.8; $P = .021$).

Conclusions—Lung ultrasound can represent an effective tool for monitoring and stratifying the prognosis of patients with SARS-CoV-2 pulmonary involvement.

Key Words—B-line; consolidations; lung ultrasound; severe acute respiratory syndrome coronavirus 2 pneumonia; vertical artifacts

Since its emergence in Wuhan, Hubei province, China, in December 2019,¹ severe acute respiratory syndrome coronavirus 2 (SARS-CoV-2) infection has rapidly spread all over the world, affecting more than 21 million patients and causing

more than 760,000 deaths up to August 16, 2020.² The clinical features of coronavirus disease 2019 (COVID-19) are various, ranging from an asymptomatic/mild state to severe pneumonia, diffuse alveolar damage, and consolidations with multiorgan dysfunction.³ Thus, it is crucial to diagnose and monitor pneumonia in patients with COVID-19 to identify worsening cases.

Chest computed tomography (CT) plays a pivotal role in timely detection of lung abnormalities, which largely consist of mainly patchy (confluent in the late stages) bilateral lesions with a peripheral or posterior distribution, appearing as pure ground glass opacity, ground glass opacity with reticular or interlobular septal thickening, a crazy-paving pattern, and consolidation, without pleural effusion.⁴ However, despite its utility, CT is not readily available in many resource-limited settings and cannot be extensively used in an epidemic context or in an environment with limited resources.

Lung ultrasound (LUS) gives better results compared to standard chest radiography for evaluating pneumonia and acute respiratory distress syndrome, with the added advantage of ease of its use at the point of care, its repeatability, absence of radiation exposure, and low cost.⁵ Moreover, LUS was found to be an important tool for the rapid evaluation and assessment of the pulmonary status in patients during the 2001 H1N1⁶ and 2013 avian influenza A (H7N9) epidemics.⁷ Since the outbreak, several studies have emerged in the literature evaluating the use of LUS in patients with confirmed COVID-19.^{8,9} Therefore, LUS was proposed as a diagnostic and follow-up modality in patients with COVID-19, and a standardized approach regarding equipment and the acquisition protocol, with a scoring system for severity classification,¹⁰ was developed. The aim of this study was to propose a new LUS score and evaluate its correlation with clinical and laboratory findings and with the outcome of patients with COVID-19 admitted in the Department of Internal Medicine of the San Matteo Hospital in Pavia (Lombardy, northern Italy).¹¹ Especially, we aimed to verify whether this new LUS score, integrated with the clinical evaluation, could help physicians in identifying worsening patients to improve the diagnostic and therapeutic management of this new infection.

Materials and Methods

The study was approved by our local Institutional Review Board (protocol 20200063762), and written informed consent was obtained from all study participants. Ninety-five patients suspected of having SARS-CoV-2 infection because of fever and respiratory symptoms, such as cough and dyspnea, were admitted from March 15 to April 29, 2020, into the internal medicine ward of the San Matteo Hospital. Inclusion criteria were age 18 years or older, confirmed COVID-19 infection based on the detection of SARS-CoV-2 on a reverse transcriptase polymerase chain reaction from a nasopharyngeal swab or bronchoalveolar wash, and a collaborative status allowing them to express informed consent. Patients were excluded if they were not able to express their consent, if they were severely obese (body mass index [BMI] >35 kg/m²), or if they were affected by heart failure or interstitial lung disease, such as usual interstitial pneumonia or lung fibrosis secondary to rheumatologic disease.

A LUS examination was performed by an expert physician (>15 years of experience in thoracic ultrasound [US]) on the day of admission in the department (t-0), and a second LUS examination (t-1) was repeated after a mean of 10 days from admission. A MyLab Sat US system (Esaote SpA, Genoa, Italy) equipped with a convex transducer (3.5–5 MHz) was used for the US study, using an abdominal setting and fixing a standard 10-cm depth. A single-focal-point modality was used, setting the focal point on the pleural line. Patients were evaluated by a standard sequence of US scans in 14 anatomic chest landmarks,¹⁰ with intercostal scans, to cover the widest surface possible with a single scan, avoiding costal shadows. Landmarks ranging from 1 to 6 referred to dorsal areas. Landmarks ranging from 7 to 10 referred to lateral areas. Finally, landmarks ranging from 11 to 14 referred to the anterior chest wall. For each landmark a 10-second video clip was registered to document the grade of the lung involvement and for subsequent revision. A LUS scoring system ranging from 0 to 3^{10,12,13} was reported for every single scan:

- Score 0: the pleural line is continuous and regular. Horizontal artifacts are present (A-lines). They indicate the high reflectivity of the normally aerated

lung surface and characterize the visual representation of the multiple reflections between the US transducer and the lung surface itself.

- Score 1: the pleural line is indented but shows slight alterations (small interruptions). Sporadic vertical artifacts are present, assuming the appearance of bright B-lines or small bands of white lung. This appearance is due to local alterations in the acoustic properties of the lung, caused by variations in subpleural tissue density and geometry. This phenomenon may open channels accessible to US, which can explain the appearance of the vertical artifacts.
- Score 2: the pleural line has relevant alterations and appears focally broken. Below the breaking point, vertical artifacts and white lung are predominant. Small consolidated subpleural areas (darker areas) can be present. These consolidations signal the loss of aeration and the transition of these areas toward acoustic properties similar to soft tissue rather than the aerated lung. A characteristic image is the appearance of areas of white lung deep to the consolidations. This highly scattering environment can explain this peculiar pattern (Figure 1).
- Score 3: the pleural line is highly irregular and cobble. The scanned areas show dense and largely

extended white lung with or without larger consolidations (Figure 2).

Clips were examined a second time by the same physician who performed the examination, who was blinded to clinical outcomes. The highest score resulting from each landmark was reported, and a total LUS score was calculated as the sum of the scores at each explored area. Pleural effusion was evaluated too. Laboratory assessments of the patients consisted of a complete blood count, coagulation tests, renal and liver function, ferritin, C-reactive protein, lactate dehydrogenase (LDH), interleukin 6 dosage, and an arterial blood gas analysis.

A worsening evolution was defined by major clinical outcomes consisting of high-flow oxygen support, intensive care unit (ICU) admission, and death. High-flow oxygen support was defined by the use of a continuous positive airway pressure helmet or need for invasive ventilation.

The primary investigated end point was the association between the LUS score severity and worsening. Secondary end points were the change in the total LUS score at discharge and the association between the LUS score and clinical characteristics (symptoms, comorbidities, age, and BMI) and laboratory data (arterial blood gas analysis, routine blood tests, inflammatory indices, and D-dimer).^{14–16}

For the statistical analysis, Stata version 16 software (StataCorp, College Station, TX) was used. Two-sided $P < .05$ was considered statistically significant. We summarized continuous data by the mean and standard deviation and the median and 25th to 75th percentiles and categorical data as counts and percentages. For the purpose of the analysis, we dichotomized the total LUS score at its median (≤ 24 or > 24), as well as the number of segments with scores 2 and 3 (≤ 8 or > 8) and the number of segments with score 3 (≥ 3 or > 3).

Logistic regression was used to assess the univariable association of the overall score and the incidence of the different comorbidities and the multivariable association with adjustment for the number of comorbidities (> 2), age (> 65 years), sex (male) and BMI (≥ 25 kg/m²). Odds ratios (ORs) and 95% confidence intervals (CIs) were reported. We computed the model area under the receiver operating characteristic curve for discrimination. The

Figure 1. Pattern 2 with typical vertical artifacts and subpleural micronodules.

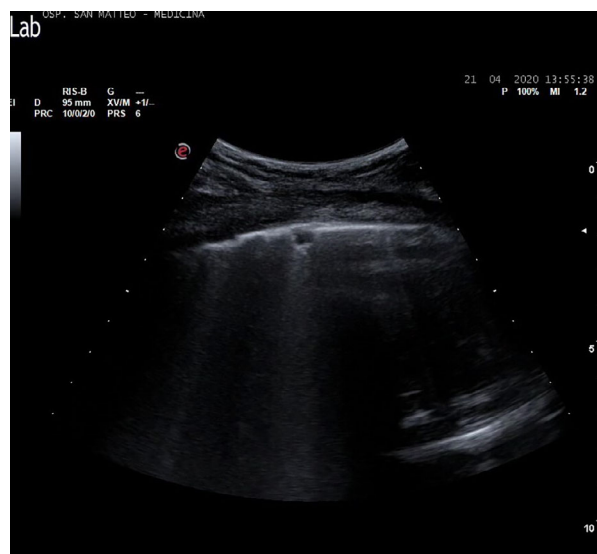


Figure 2. Pattern 3 with vertical confluent artifacts and large confluent consolidations.



probability of worsening from the logistic model and 95% CI was derived and plotted against the score to create a nomogram for practical use. Wilcoxon and McNemar tests were used to compare continuous and dichotomized scores over time, respectively. Finally, we used the Spearman *R* (95% CI) to assess the correlation of the score with continuous variables and the Student *t* test to compare the score over categorical variables.

Results

From March 15 to April 29, 2020, 52 of 95 consecutive patients with SARS-CoV-2 infection confirmed by a nasopharyngeal swab or bronchoalveolar washing were enrolled. Forty-three patients were excluded for the presence of exclusion criteria. The mean age was 63.6 ± 16.8 years (range, 26–92 years); 23 patients (44.2%) were older than 65 years; and 28 patients (53.8%) were men. Of these patients, 30 (57.7%) had a BMI higher than 25 kg/m^2 , with 5 higher than 30 kg/m^2 .

Among the 52 patients enrolled, 38 (73%) had 2 or fewer coexisting medical conditions. Hypertension (51.9%), cardiovascular disease (28.8%), chronic kidney disease (25%), diabetes (19.2%), and active

cancer (15%) were the most common coexisting conditions. The most common symptoms at presentation were fever (88.4%), dyspnea (61.5%), dry cough (51.9%), and gastrointestinal symptoms (19.2%; Table 1). Chest radiography revealed bilateral lung consolidations with ground glass opacity, nodules, and reticular-nodular opacities in 46 patients (88%); the remaining (6 patients [12%]) showed negative chest radiographic findings.

The mean hospital stay was 19 days. The first LUS examination on the day of the admission in the department (t-0) was performed in all the 52 patients. Because of rapid and unexpected worsening (death or admission to the ICU), only 24 patients (46%) had a second LUS evaluation (t-1).

At the LUS examination, peripheral and lower zones were the most common regions affected, with equal distributions in both sides, as shown in Figure 3. Anterior and superior lateral-posterior lung fields were less involved.

Among the 52 patients enrolled, 25 (48%) showed pleural effusion, and in 13 of these 25 patients (52%), the effusion was bilateral; 6 (24%) showed monolateral effusion on the left side and 6 (24%) on the right side. Twenty-five patients had a total LUS score higher than 24 (48%), whereas 25 patients had more than 3 segments with score 3 (48%), and 24 patients had more than 8 segments with scores 2 and 3 (46%).

Primary End Point

During the admission period, a worsening outcome, established as a combination of high-flow oxygen support, ICU admission, and death, was observed in 20 (39%) patients. Particularly, 16 patients (30.7%) required treatment with a continuous positive airway pressure helmet; 7 (13.4%) were admitted to the ICU; and 8 died (15%). The total mean LUS scores were 20.4 ± 8.5 and 29.2 ± 7.3 in patients without and with worsening, respectively.

In the univariable analysis, the total LUS score at admission was associated with higher odds of worsening both on a continuous scale (OR, 1.14; 95% CI, 1.05 to 0.24; $P = .002$) and when considering the number of segments with score 3, dichotomized at its median value of 3 (>3 segments with LUS score 3, OR, 6.30; 95% CI, 1.78 to 22.24; $P = .004$). In the multivariable analysis, adjusted for comorbidities

Table 1. Patient Characteristics (n = 52)

Characteristic	Value
Age, y	63.6 ± 16.8
Female	24 (46.2)
Male	28 (53.8)
BMI, kg/m ²	25.3 ± 3.7
Positive nasal swab result	51 (99)
Positive bronchoalveolar wash result	1 (1)
Comorbidities	
Hypertension	27 (51.9)
Cardiovascular disease	15 (28.8)
Diabetes	10 (19.2)
Chronic obstructive pulmonary disease	9 (17)
Interstitial lung disease	0 (0)
Active cancer	8 (15)
Autoimmune disease	5 (9)
Chronic kidney disease	13 (25)
Symptoms	
Fever	46 (88.4)
Cough	27 (51.9)
Shortness of breath	32 (61.5)
Thoracic pain	4 (8)
Diarrhea/vomiting	10 (19.2)
Anosmia	2 (4)
Ageusia	3 (6)
Laboratory results	
C-reactive protein, mg/dL	10.20 ± 8.1
Po ₂ , mm Hg	80 ± 28.2
Po ₂ -to-Fio ₂ ratio, mm Hg	247.5 ± 114.6
LDH, U/L	334 ± 109.6
D-Dimer, ng/mL	2940 ± 4795.8
Ferritin, ng/mL	939.6 ± 1044.9
Lymphocytes, x10 ³ /μL	0.91 ± 0.5
Albumin, g/dL	2.9 ± 0.5
Interleukin 6, pg/mL	78.5 ± 63

Data are presented as mean ± SD and number (percent) where applicable.

(>2), age (>65 years), sex, and BMI (≥25 kg/m²), the association between the total LUS score and worsening (OR, 1.17; 95% CI, 1.05 to 1.29; *P* = .003) was confirmed. The model showed good discrimination (area under the receiver operating characteristic curve, 0.82). Figure 4 provides a nomogram for the prediction of the probability of worsening given the score. Moreover, a total median LUS score higher than 24 was associated with an almost 6-fold increase in the odds of worsening (OR, 5.67; 95% CI, 1.29 to 24.8; *P* = .021).

Secondary End Points

The proportion of severe cases, defined by more than 3 segments with LUS score 3, decreased significantly at t-1 (from 50% to 42%; *P* < .001), as well as the proportion of patients with more than 8 segments with LUS scores 2 and 3 (from 50% to 33%; *P* < .001). A strong correlation between the total LUS score and Po₂-to-Fio₂ ratio (*R* = −0.83; 95% CI, −0.90 to −0.71; *P* < .001; Figure 5) was observed, whereas the correlation between the LUS score and D-dimer (*R* = 0.52; 95% CI, 0.29 to 0.70; *P* < .001) and LDH (*R* = 0.52; 95% CI, 0.29 to 0.70; *P* < .001) was moderate. The correlation between the total LUS score and Po₂ (*R* = −0.35; 95% CI, −0.57 to −0.08; *P* = .011) and ferritin (*R* = 0.28; 95% CI, 0.01 to 0.52; *P* = .041) was weak. There was no association between the LUS score and lymphocyte count, albumin level, interleukin 6 level, and C-reactive protein. Finally, pleural effusion was associated with a higher

Figure 3. Percentage distribution of score 3 on lung fields.

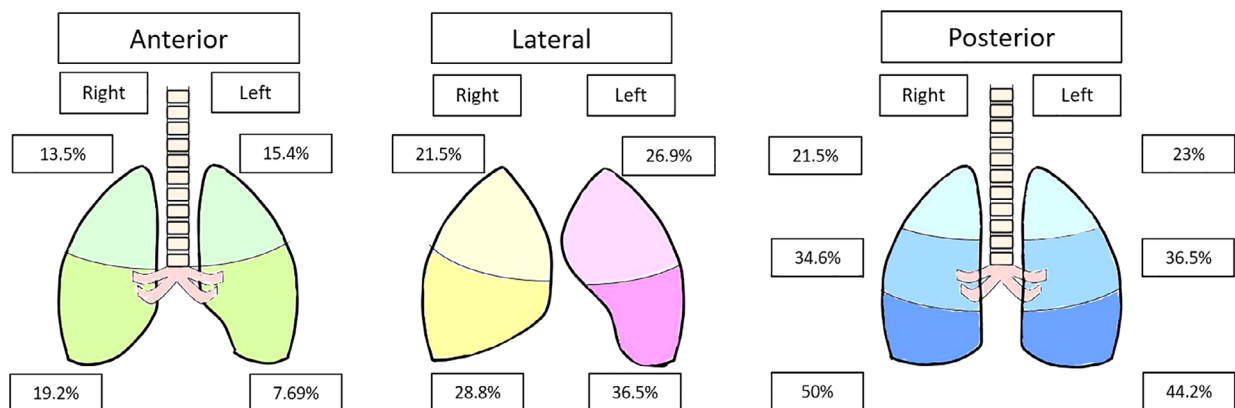
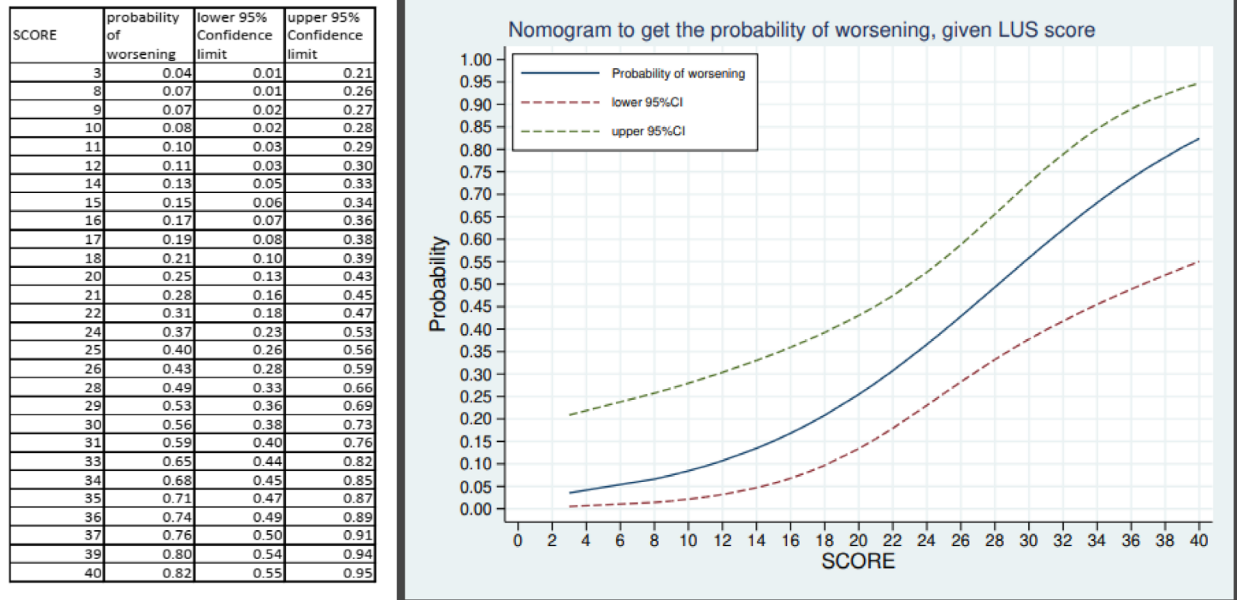


Figure 4. Nomogram to compute the probability of worsening given the score (solid blue line), together with its 95% CI (dashed red lines).



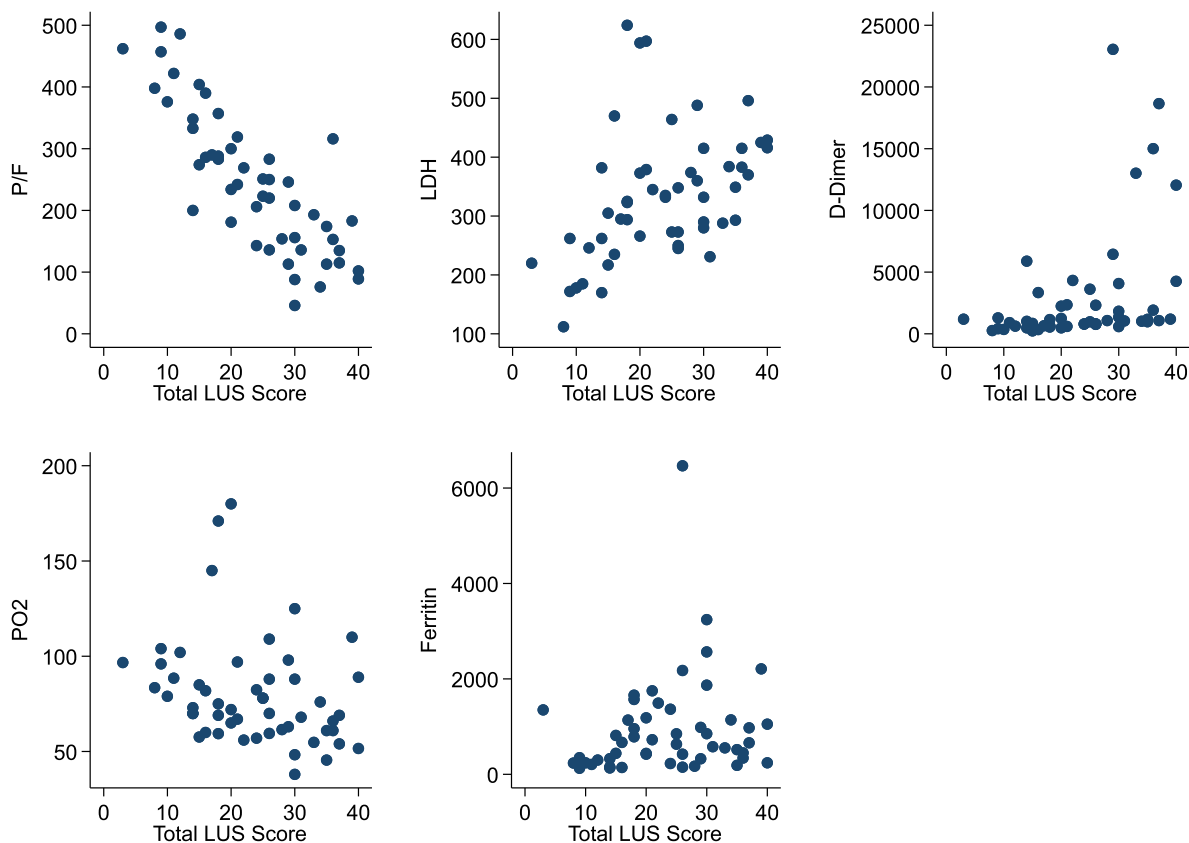
total LUS score (20.0 ± 9.2 versus 27.2 ± 8.4 ; $P = .005$; difference, 7.2; 95% CI, 2.3 to 12.1).

Discussion

It has been shown that COVID-19 pulmonary involvement has evolutive phenotypes.¹⁷ Diffuse alveolar damage represents the first step, followed by consolidative events, probably related to an immune-mediated reaction, including microvascular damage.^{18–21} The characteristic target of COVID-19 in the lung is the peripheral pulmonary tissue²² and the posterobasal and laterobasal areas are the most involved. Lung US is an optimal tool for exploring tissue density and subpleural inhomogeneities of the lung.²³ Because diffuse alveolar damage, ground glass and septal CT opacities, and subpleural consolidations represent physical densities involving the tissue devoted to gas exchanges, LUS has a strong theoretical advantage for the study of the superficially diseased lung and its evolutionary behavior.^{4,5} The current evidence states that nonconsolidative lung densities appear on LUS images as vertical artifacts

erasing the specular appearance of the normal lung (characterized by the so-called A-lines).^{24–26} Probably, these artifacts (generically named B-lines) are the end result of entrapment of the acoustic energy inside channels (acoustic traps) appearing along the pleural surface and caused by a variation (increase) of the full-to-empty ratio of the subpleural lung. The traps may act as a secondary US source, and part of the trapped energy is reradiated to the transducer across the entry and exit of the trap.²⁷ The visual result is vertical artifacts showing a variable brightness, length, width, and organization along the pleural line.²⁴ Finally, the generation of an artifact may involve either only a single trap at a time, as in the case of an isolated B-line, or multiple smaller acoustic traps, as in the case of white lung.^{27,28} This sign suggests the presence of a relatively homogeneous scattered distribution (many small air spaces close to each other, which contribute to the formation of many small acoustic traps), which gives rise to numerous multiple reflections. Between these 2 patterns, a great variety of artifacts exist, signaling a variable nonconsolidative density of the subpleural pulmonary tissue and therefore variable gravity of the diseased lung. Lung

Figure 5. Scatterplots showing the correlation of the total LUS score with laboratory findings. *R* and 95% CI values are reported in “Results.”



consolidations represent a heavily deaerated subpleural pulmonary area, and in this case, their US appearance is similar to a solid organ.^{26,27,29}

The LUS score (0–3) used in this study is based on these premises and on previous studies,¹⁰ according to the hypothesis that a greater extension of the involved lung areas could be correlated with greater pathophysiologic impairment of a patient with COVID-19. As seen to date, the timely classification and monitoring of patients with SARS-CoV-2 are essential for a good outcome of the disease, and it appears to be even more so during the pandemic, in which the excessive influx of patients in hospitals can put an organization in a situation of crisis and affect the efficiency of the services of the wards and emergency departments.

Unlike the LUS score used in the emergency department or ICU,³⁰ the score used in this study

adds 2 additional posterior thoracic scans to better evaluate the lung fields most involved in SARS-CoV-2 pneumonia. Our score may estimate the probability of worsening of a patient with SARS-CoV-2 pneumonia and predict a possible evolution of the disease, since the total LUS score correlates with worsening.

Our results confirm the validity of the score system for classifying pulmonary involvement in patients with COVID-19. The total LUS score is associated with established end points of clinical worsening, including high-flow oxygen support, ICU admission, and death. Particularly, the odds of worsening are independent of the demographic and clinical characteristics of patients with COVID-19. According to our data, a nomogram (Figure 4) that easily allows estimation of the probability of worsening given the total LUS score at the bedside may be produced, and

this is, in our opinion, important because of the variable, more-or-less evolutionary, characteristics of COVID-19 lung involvement.

We were also able to show that higher total LUS scores are associated with some clinical and laboratory findings and, in particular, with the presence of pleural effusion, with a lower PO_2 -to- FiO_2 ratio and a high level of LDH. The D-dimer and LDH also have a moderate correlation with the total score, suggesting the hypothesis of a possible not-only inflammatory but also thrombotic nature of lung involvement.²¹

In the subgroup of patients in whom a second LUS examination was performed (t-1), we were able to show that the proportion of patients with more severe disease (segmental scores 2 and 3) decreased significantly, underlining the importance of LUS for patient monitoring. In our population, the most severe LUS cases were patients with a total score higher than 24, showing more than 3 segments with score 3 or more than 8 segments with score 2 or 3. The typical distribution of score 3 was gravitational, preferring the basal fields, especially posterior and lateral, where the ventilation-to-perfusion ratio is lower, comparable to the findings of previous studies that used CT as imaging.^{4,18} Particular attention should be paid to patients who have more than 3 segments with LUS score 3, who have odds of worsening 6.3 times greater than the rest of the patients, as well as an LUS score higher than 24 (OR, 5.67).

Although pleural effusion is not considered a significantly representative sign of COVID-19, in our experience, it is often associated with more severe cases. Interestingly, we observed a high prevalence of pleural effusion compared to other studies,^{4,18,31} and this finding was probably related to the high sensitivity of LUS for detecting small pleural effusion compared to radiography. Anyway, from a pathophysiologic point of view, it is sufficiently clear that areas showing vertical artifacts and, in particular, white lung may represent hypoventilated and perhaps hyperfused pulmonary tissue,³² thus acting on blood gases through a shunt mechanism, whereas highly hypoperfused consolidated areas contribute to the global shunt effect, diverting the blood to the hyperperfused regions.^{21,26,27,29}

The results of this study are in agreement with the already-described concept of the evolutionary characteristics of COVID-19 pulmonary involvement,

in which some patients may progress from directly virus-related pulmonary damage (diffuse alveolar damage) to more complex conditions consisting of organizing pneumonia, resorptive activity (crazy-paving pattern), and consolidative events, with or without perfusion defects.^{20,24} The reason many patients do not develop this evolutionary pattern is under investigation, but the involvement of the immune system is particularly intriguing.^{21,33}

The limits of the study were the modest sample population, which did not allow the correct identification of an optimal total score cutoff, the LUS examination performed at a variable distance from the onset of disease, and the control US examination (t-1) that was repeated after a short interval from the first examination (although not less than 1 week) in a subset of patients only. Moreover, CT was not used, considering not only the excessive radiation exposure, especially to younger patients, but also the mandatory scanner disinfection procedures that have to take place, and overall, because of the huge number of critical patients who arrived at the hospital.

In conclusion, the LUS protocol that we propose appears to be a valuable tool in medium- to low-intensity care units to predict the probability of clinical worsening of SARS-CoV-2 pneumonia, to identify the most appropriate therapeutic and managerial path for the patients, and to establish an adequate follow-up to monitor the progress of the disease.

References

1. Lu H, Stratton CW, Tang YW. Outbreak of pneumonia of unknown etiology in Wuhan, China: the mystery and the miracle. *J Med Virol* 2020; 92:401–402.
2. World Health Organization. *Novel Coronavirus (2019-nCoV)*. Geneva, Switzerland: World Health Organization; 2020.
3. Wu Z, McGoogan JM. Characteristics of and important lessons from the coronavirus disease 2019 (COVID-19) outbreak in China: summary of a report of 72,314 cases from the Chinese Center for Disease Control and Prevention. *JAMA* 2020; 323:1239–1242.
4. Song F, Shi N, Shan F, et al. Emerging 2019 novel coronavirus (2019-nCoV) pneumonia. *Radiology* 2020; 295:210–217.
5. Chiumello D, Umbrello M, Sferazza Papa GF, et al. Global and regional diagnostic accuracy of lung ultrasound compared to CT

- in patients with acute respiratory distress syndrome. *Crit Care Med* 2019; 47:1599–1606.
6. Testa A, Soldati G, Copetti R, Giannuzzi R, Portale G, Gentiloni-Silveri N. Early recognition of 2009 pandemic influenza A (H1N1) pneumonia by chest ultrasound. *Crit Care* 2012; 16:R30.
 7. Zhang YK, Li J, Yang JP, Zhan Y, Chen J. Lung ultrasonography for the diagnosis of 11 patients with acute respiratory distress syndrome due to bird flu H7N9 infection. *Virol J* 2015; 12:176.
 8. Buonsenso D, Piano A, Raffaelli F, Bonadia N, de Gaetano Donati K, Franceschi F. Point-of-care lung ultrasound findings in novel coronavirus disease-19 pneumoniae: a case report and potential applications during COVID-19 outbreak. *Eur Rev Med Pharmacol Sci* 2020; 24:2776–2780.
 9. Yasukawa K, Minami T. Point-of-care lung ultrasound findings in patients with COVID-19 pneumonia. *Am J Trop Med Hyg* 2020; 102:1198–1202.
 10. Soldati G, Smargiassi A, Inchingolo R, et al. Proposal for international standardization of the use of lung ultrasound for patients with covid-19: a simple, quantitative, reproducible method. *J Ultrasound Med* 2020; 39:1413–1419.
 11. Lenti MV, Corazza GR, Di Sabatino A. Carving out a place for internal medicine during COVID-19 epidemic in Italy. *J Intern Med* 2020; 288:263–265.
 12. Soldati G, Smargiassi A, Inchingolo R, et al. Is there a role for lung ultrasound during the COVID-19 pandemic? *J Ultrasound Med* 2020; 39:1459–1462.
 13. Soldati G, Smargiassi A, Inchingolo R, et al. On lung ultrasound patterns specificity in the management of COVID-19 patients. *J Ultrasound Med*. 2020;39(11):2883–2884.
 14. Huang C, Wang Y, Li X, et al. Clinical features of patients infected with 2019 novel coronavirus in Wuhan, China. *Lancet* 2020; 395:497–506.
 15. Wang D, Hu B, Hu C, et al. Clinical characteristics of 138 hospitalized patients with 2019 novel coronavirus–infected pneumonia in Wuhan, China. *JAMA* 2020; 323:1061–1069.
 16. Chen N, Zhou M, Dong X, et al. Epidemiological and clinical characteristics of 99 cases of 2019 novel coronavirus pneumonia in Wuhan, China: a descriptive study. *Lancet* 2020; 395:507–513.
 17. Gattinoni L, Chiumello D, Caironi P, et al. COVID-19 pneumonia: different respiratory treatments for different phenotypes? *Intensive Care Med* 2020; 46:1099–1102.
 18. Xu X, Yu C, Qu J, et al. Imaging and clinical features of patients with 2019 novel coronavirus SARS-CoV-2. *Eur J Nucl Med Mol Imaging* 2020; 47:1275–1280.
 19. Konopka KE, Nguyen T, Jentzen JM, et al. Diffuse alveolar damage (DAD) from coronavirus disease 2019 infection is morphologically indistinguishable from other causes of DAD. *Histopathology* 2020; 77:570–578.
 20. Zhang T, Sun LX, Feng RE. Comparison of clinical and pathological features between severe acute respiratory syndrome and coronavirus disease 2019 [in Chinese]. *Zhonghua Jie He Jibe Hu Xi Za Zhi* 2020; 43:496–502.
 21. Soldati G, Giannasi G, Smargiassi A, et al. Contrast-enhanced ultrasound in patients with COVID-19: pneumonia, acute respiratory distress syndrome, or something else? *J Ultrasound Med*. 2020:10. <https://doi.org/10.1002/jum.15338>.
 22. Pan F, Ye T, Sun P, et al. Time course of lung changes at chest CT during recovery from coronavirus disease 2019 (COVID-19). *Radiology* 2020; 295:715–721.
 23. Soldati G, Smargiassi A, Demi L, Inchingolo R. Artfactual lung ultrasonography: it is a matter of traps, order, and disorder. *Appl Sci* 2020; 10:1570.
 24. Lichtenstein DA, Mézière GA, Biderman P, Gepner A, Barré O. The comet-tail artifact: an ultrasound sign of alveolar-interstitial syndrome. *Am J Respir Crit Care Med* 1997; 156:1640–1646.
 25. Soldati G, Demi M, Inchingolo R, Smargiassi A, Demi L. On the physical basis of pulmonary sonographic interstitial syndrome. *J Ultrasound Med* 2016; 35:2075–2086.
 26. Soldati G, Demi M, Smargiassi A, Inchingolo R, Demi L. The role of ultrasound lung artifacts in the diagnosis of respiratory diseases. *Exp Rev Respir Med* 2019; 13:163–172.
 27. Demi M, Prediletto R, Soldati G, Demi L. Physical mechanisms providing clinical information from ultrasound lung images: hypotheses and early confirmations. *IEEE Trans Ultrason Ferroelectr Freq Control* 2020; 67:612–623.
 28. Soldati G, Copetti R, Sher S. Sonographic interstitial syndrome: the sound of lung water. *J Ultrasound Med* 2009; 28:163–174.
 29. Soldati G, Smargiassi A, Mariani AA, Inchingolo R. Novel aspects in diagnostic approach to respiratory patients: is it the time for a new semiotics? *Multidiscip Respir Med* 2017; 12:15.
 30. Tung-Chen Y, Martí de Gracia M, Diez-Tascón A, et al. Correlation between chest computed tomography and lung ultrasonography in patients with coronavirus disease 2019 (COVID-19). *Ultrasound Med Biol* 2020; 46:2918–2926.
 31. Sultan LR, Sehgal CM. A review of early experience in lung ultrasound in the diagnosis and management of COVID-19. *Ultrasound Med Biol* 2020; 46:2530–2545.
 32. Lang M, Som A, Mendoza DP, et al. Hypoxaemia related to COVID-19: vascular and perfusion abnormalities on dual-energy CT [published online ahead of print April 30, 2020]. *Lancet Infect Dis*. 2020;S1473-3099(20):30367–4.
 33. Allegra A, Di Gioacchino M, Tonacci A, Musolino C, Gangemi S. Immunopathology of SARS-CoV-2 infection: immune cells and mediators, prognostic factors, and immune-therapeutic implications. *Int J Mol Sci* 2020; 21:4782.